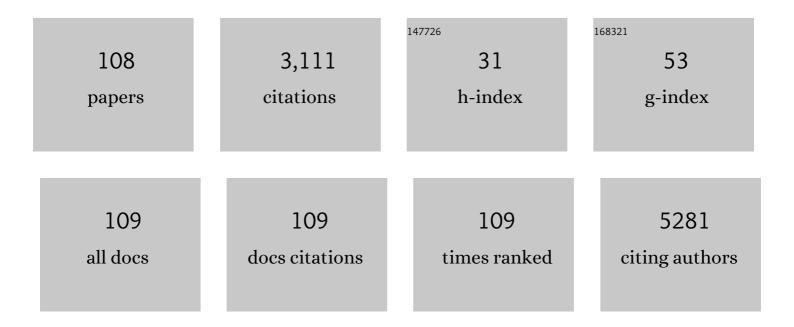
List of Publications by Year in descending order

Source: https://exaly.com/author-pdf/2965734/publications.pdf Version: 2024-02-01



#	Article	IF	CITATIONS
1	Anion intercalation pseudo-capacitance performance of oxygen-deficient double perovskite prepared via facile wet chemical route. Materials Science in Semiconductor Processing, 2022, 138, 106300.	1.9	4
2	An extensive study of depth dose distribution and projectile fragmentation cross-section for shielding materials using Geant4. Applied Radiation and Isotopes, 2022, 180, 110068.	0.7	2
3	Engineered perovskite LaCoO3/rGO nanocomposites for asymmetrical electrochemical supercapacitor application. Journal of Materials Science: Materials in Electronics, 2022, 33, 2590-2606.	1.1	14
4	Excellent microwave absorbing performance of biomass-derived activated carbon decorated with <i>in situ</i> -grown CoFe ₂ O ₄ nanoparticles. Materials Advances, 2022, 3, 2533-2545.	2.6	6
5	Quality of Local Scale Surface Weather Analogs in Two Climatologically and Geographically Distinct Mountainous Regions. Meteorology and Atmospheric Physics, 2022, 134, 1.	0.9	0
6	Biomass-Derived Activated Carbon/Epoxy Composite as Microwave Absorbing Material. Journal of Electronic Materials, 2022, 51, 2918-2925.	1.0	7
7	Organoamine Templated Multifunctional Hybrid Metal Phosphonate Frameworks: Promising Candidates for Tailoring Electrochemical Behaviors and Size-Selective Efficient Heterogeneous Lewis Acid Catalysis. Inorganic Chemistry, 2022, 61, 9580-9594.	1.9	11
8	Excellent microwave absorbing and electromagnetic shielding performance of grown MWCNT on activated carbon bifunctional composite. Carbon, 2022, 198, 151-161.	5.4	18
9	Analog ensembleÂ(AE) systems for real time quantitative precipitation forecasts (QPFs) for different forecast lead times at local scale over the north-westÂHimalaya (NWH), India. Meteorology and Atmospheric Physics, 2021, 133, 533-552.	0.9	3
10	MoS ₂ nanoparticle/activated carbon composite as a dual-band material for absorbing microwaves. Nanoscale Advances, 2021, 3, 4196-4206.	2.2	22
11	Monte Carlo simulation study for proton therapy at energy range 62â€MeV – 240â€MeV using GEANT4. AIP Conference Proceedings, 2021, , .	0.3	0
12	Activated carbon derived from mango leaves as an enhanced microwave absorbing material. Sustainable Materials and Technologies, 2021, 27, e00244.	1.7	17
13	L-cysteine functionalized graphene quantum dots for sub-ppb detection of As (III). Nanotechnology, 2021, 33, .	1.3	1
14	Study of photoluminescence and nonlinear optical behaviour of AgCu nanoparticles for nanophotonics. Nano Structures Nano Objects, 2021, 28, 100807.	1.9	11
15	Symmetric/asymmetric energy storage device of reduced graphene oxide assisted LaNi0.9Co0.1O3 perovskite nanomaterials. Applied Physics A: Materials Science and Processing, 2021, 127, 1.	1.1	2
16	Novel green photo-catalyst â€~turmeric roots' for pesticides degradation: Preparation and characterizations. Materials Letters, 2020, 262, 127030.	1.3	10
17	Computational study of fragmentation cross-sections for 28Si ions in various media using GEANT4. Nuclear Instruments & Methods in Physics Research B, 2020, 464, 5-11.	0.6	1
18	Phase transformation in wet chemically synthesized Y2NiFeO6, and its magnetic and energy storage properties. Applied Physics A: Materials Science and Processing, 2020, 126, 1.	1.1	6

#	Article	IF	CITATIONS
19	Structural, Dielectric, and Energy Storage Properties of Citric Acid and Ethylene Glycol Assisted Hydrothermally Synthesized Y ₂ FeCoO ₆ . Physica Status Solidi (A) Applications and Materials Science, 2020, 217, 2000324.	0.8	6
20	Modification in mechanical, tribological & electrical properties of epoxy at low weight fraction of multiwalled carbon nanotube. Materials Today: Proceedings, 2020, 26, 1836-1840.	0.9	5
21	The synthesis, structural, optical and electrical characterizations of double perovskite oxide Y2CuCoO5. AIP Conference Proceedings, 2020, , .	0.3	0
22	Fragmentation cross-section study of 28Si ions on 12C target with simulation toolkit GEANT4. AIP Conference Proceedings, 2020, , .	0.3	0
23	Energy storage properties of double perovskites Gd2NiMnO6 for electrochemical supercapacitor application. Solid State Sciences, 2020, 105, 106252.	1.5	34
24	Effect of calcinations on structural, optical and photocatalytic properties of a green photo-catalyst â€~turmeric roots powder'. Optik, 2020, 216, 164804.	1.4	3
25	Effect of Nanographite on Electrical Mechanical and Wear Characteristics of Graphite Epoxy Composites. Defence Science Journal, 2020, 70, 306-312.	0.5	10
26	Quality of local scale surface weather analogs over the north-west Himalaya (NWH), India. Journal of Earth System Science, 2019, 128, 1.	0.6	1
27	Spatio-temporal variability of binary weather patterns and precipitation amounts of short time intervals during winter period over the north-west Himalaya (NWH). Journal of Earth System Science, 2019, 128, 1.	0.6	1
28	Enhanced microwave absorption properties of Co and Ni co-doped iron (II,III)/reduced graphene oxide composites at X-band frequency. Journal of Materials Science: Materials in Electronics, 2019, 30, 19325-19334.	1.1	13
29	Enhanced photocatalytic performance of m-WO3 and m-Fe-doped WO3 cuboids synthesized via sol-gel approach using egg albumen as a solvent. Materials Science in Semiconductor Processing, 2019, 104, 104690.	1.9	29
30	Investigation of structural, optical and photocatalytic properties of W(0.99)Pd(0.01)O3 nanoparticles. AIP Conference Proceedings, 2019, , .	0.3	0
31	The impacts of the approaching western disturbances (WDs) on the surface meteorological variables over the north-west Himalaya (NWH), India. Journal of Earth System Science, 2019, 128, 1.	0.6	2
32	Microstructural evolution and photoluminescence performanance of nickel and chromium doped ZnO nanostructures. Materials Chemistry and Physics, 2018, 205, 9-15.	2.0	10
33	Multifunctional silanized silica nanoparticle functionalized graphene oxide: polyetherimide composite film for EMI shielding applications. Journal of Materials Science: Materials in Electronics, 2018, 29, 14122-14131.	1.1	8
34	Facile synthesis of bulk SnO 2 and ZnO tetrapod based graphene nanocomposites for optical and sensing application. Materials Chemistry and Physics, 2017, 201, 372-383.	2.0	10
35	Synthesis of N and F co-doped TiO2 nanophotocatalysts for degradation of malathion in water. Research on Chemical Intermediates, 2017, 43, 387-399.	1.3	12
36	Experimental measurements of acoustical properties of snow and inverse characterization of its geometrical parameters. Applied Acoustics, 2016, 101, 15-23.	1.7	13

#	Article	IF	CITATIONS
37	The photocatalytic investigation of methylene blue dye with Cr doped zinc oxide nanoparticles. AIP Conference Proceedings, 2015, , .	0.3	1
38	Impedance modeling for classification of flavored green teas. Turkish Journal of Electrical Engineering and Computer Sciences, 2015, 23, 2208-2214.	0.9	2
39	Effect of NaOH molar concentration on morphology, optical and ferroelectric properties of hydrothermally grown CuO nanoplates. Materials Science in Semiconductor Processing, 2015, 38, 72-80.	1.9	57
40	Effect of NaOH molar concentration on optical and ferroelectric properties of ZnO nanostructures. Applied Surface Science, 2015, 356, 438-446.	3.1	37
41	Acoustic emission characteristics and b-value estimate in relation to waveform analysis for damage response of snow. Cold Regions Science and Technology, 2015, 119, 170-182.	1.6	33
42	Effect of Sr2+, Ba 2+ and Ta5+ lons on Structural and Electrical Properties of BNKT Ceramics. Materials Today: Proceedings, 2015, 2, 2784-2788.	0.9	1
43	Structural and optical studies of CuO nanostructures. , 2014, , .		1
44	Investigation of variation of energy of laser beam on structural, electrical and optical properties of pulsed laser deposited CuO thin films. , 2014, , .		0
45	Photocatalytic degradation of methylene blue with Cu doped ZnS nanoparticles. Journal of Luminescence, 2014, 145, 6-12.	1.5	128
46	Structural and optical study of Li doped CuO thin films on Si (100) substrate deposited by pulsed laser deposition. Applied Surface Science, 2014, 307, 280-286.	3.1	105
47	Growth of thermally evaporated SnO2 nanostructures for optical and humidity sensing application. Sensors and Actuators B: Chemical, 2014, 201, 369-377.	4.0	31
48	Structural, optical, and ferroelectric behavior of Zn1â^'xLixO (0⩽x⩽0.09) nanostructures. Journal of Alloys and Compounds, 2014, 585, 345-351.	2.8	23
49	Multi-sensor couplers and waveguides for efficient detection of acoustic emission behavior of snow. Cold Regions Science and Technology, 2014, 101, 1-13.	1.6	12
50	The dielectric behavior of Zn1â^'xNixO/NiO two-phase composites. Journal Physics D: Applied Physics, 2014, 47, 435305.	1.3	15
51	Nickel-induced structural, optical, magnetic, and electrical behavior of α-Fe ₂ O ₃ . Physica Status Solidi (B): Basic Research, 2014, 251, 1552-1557.	0.7	10
52	Biogenesis of PbS Nanocrystals by Using Rhizosphere Fungus i.e., Aspergillus sp. Isolated from the Rhizosphere of Chickpea. BioNanoScience, 2014, 4, 189-194.	1.5	9
53	Structural, Optical, and Ferroelectric Behaviors of Cu1â^'x Li x O (0Ââ‰ÂxÂâ‰Â0.09) Nanostructures. Acta Metallurgica Sinica (English Letters), 2014, 27, 306-312.	1.5	9
54	Comparative study of depth dose-distributions and partial fragmentation cross sections of 56Fe ions on polyethylene using GEANT4. Nuclear Instruments & Methods in Physics Research B, 2014, 328, 8-13.	0.6	1

#	Article	IF	CITATIONS
55	Structural, morphological and optical study of Li doped ZnO thin films on Si (100) substrate deposited by pulsed laser deposition. Ceramics International, 2014, 40, 11915-11923.	2.3	48
56	Structural, optical and photocatalytic studies of Fe doped ZnS nanoparticles. Journal of Sol-Gel Science and Technology, 2013, 67, 376-383.	1.1	16
57	Structural, optical and ferroelectric behavior of hydrothermally grown ZnO nanostructures. Superlattices and Microstructures, 2013, 64, 331-342.	1.4	36
58	Influence of silver and graphite on zinc oxide nanostructures for optical application. Optical Materials, 2013, 35, 1335-1341.	1.7	13
59	Synthesis, structural and photocatalytic studies of Mn-doped CdS nanoparticles. Research on Chemical Intermediates, 2013, 39, 645-657.	1.3	25
60	Structural, optical and ferroelectric behavior of CuO nanostructures synthesized at different pH values. Superlattices and Microstructures, 2013, 60, 129-138.	1.4	67
61	Response of CR39 detector to 5A GeV Si14+ ions and measurement of total charge changing cross-section. Radiation Physics and Chemistry, 2013, 92, 8-13.	1.4	2
62	Visible-light photocatalytic degradation of methylene blue with Fe doped CdS nanoparticles. Applied Surface Science, 2013, 270, 655-660.	3.1	66
63	Photocatalytic degradation of methylene blue with Fe doped ZnS nanoparticles. Spectrochimica Acta - Part A: Molecular and Biomolecular Spectroscopy, 2013, 113, 250-256.	2.0	65
64	Fragmentation cross-section of 600 A MeV Si14+ ions in thick polyethylene target. European Physical Journal A, 2013, 49, 1.	1.0	7
65	Structural and optical studies of Sr and Mn doped ZnO nanoparticles. , 2013, , .		0
66	Study of optical And Ferroelectric Behavior Of ZnO Nanostructures. Advanced Materials Letters, 2013, 4, 220-224.	0.3	13
67	Photocatalytic studies of silver doped ZnO nanoparticles synthesized by chemical precipitation method. Journal of Sol-Gel Science and Technology, 2012, 63, 546-553.	1.1	55
68	Structural and optical characterization of Ag-doped TiO2 nanoparticles prepared by a sol–gel method. Research on Chemical Intermediates, 2012, 38, 1443-1453.	1.3	18
69	Structures and optical properties of Zn1â~'x Ni x O nanoparticles by coprecipitation method. Research on Chemical Intermediates, 2012, 38, 1483-1493.	1.3	17
70	Calibration of CR39 detectors with new system for Fe26+ ion beam and measurement of total charge changing cross-section in Al target. Radiation Measurements, 2012, 47, 1023-1029.	0.7	6
71	Structural and optical properties of ZnO nanoparticles synthesized at different pH values. Journal of Alloys and Compounds, 2012, 539, 174-178.	2.8	69
72	Validation of Geant4 physics models for 56Fe ion beam in various media. Nuclear Instruments & Methods in Physics Research B, 2012, 291, 7-11.	0.6	6

#	Article	IF	CITATIONS
73	Structural and photocatalytic studies of Mn doped TiO2 nanoparticles. Spectrochimica Acta - Part A: Molecular and Biomolecular Spectroscopy, 2012, 98, 256-264.	2.0	91
74	Simulation of depth–dose distributions for various ions in polyethylene medium. Advances in Space Research, 2012, 49, 1691-1697.	1.2	6
75	Structural and optical characterization of Zn doped TiO2 nanoparticles prepared by sol–gel method. Journal of Sol-Gel Science and Technology, 2012, 61, 585-591.	1.1	52
76	Study of CuO Nanoparticles Synthesized by Sol-gel Method. AIP Conference Proceedings, 2011, , .	0.3	7
77	Synthesis And Optical Properties Of Nickel Doped Zinc Oxide Nanoparticles. , 2011, , .		1
78	Study of Trapping Density in Electrical Characteristics of CdTe Thin films. , 2011, , .		1
79	Effect of In additive on the photosensitivity of glassy Se80Te20alloy. Journal of Modern Optics, 2009, 56, 1272-1275.	0.6	2
80	Fragmentation cross sections of Fe26+, Si14+ and C6+ ions of 0.3–10 on polyethylene, CR39 and aluminum targets. Nuclear Physics A, 2008, 807, 206-213.	0.6	50
81	Magnetic monopole search at high altitude with the SLIM experiment. European Physical Journal C, 2008, 55, 57-63.	1.4	44
82	Results of the search for strange quark matter and Q-balls withÂthe SLIM experiment. European Physical Journal C, 2008, 57, 525-533.	1.4	37
83	Search for intermediate mass magnetic monopoles and nuclearites with the SLIM experiment. Radiation Measurements, 2005, 40, 405-409.	0.7	15
84	Calibration of the Makrofol–DE nuclear track detector using relativistic lead ions. Radiation Measurements, 2005, 40, 433-436.	0.7	13
85	Phase transfer of platinum nanoparticles from aqueous to organic solutions using fatty amine molecules. Journal of Chemical Sciences, 2004, 116, 293-300.	0.7	34
86	Formation of platinum nanoparticles at air–water interfaces by the spontaneous reduction of subphase chloroplatinate anions by hexadecylaniline Langmuir monolayers. Journal of Colloid and Interface Science, 2004, 271, 381-387.	5.0	9
87	Variation in morphology of gold nanoparticles synthesized by the spontaneous reduction of aqueous chloroaurate ions by alkylated tyrosine at a liquid–liquid and air–water interface. Journal of Materials Chemistry, 2004, 14, 2696.	6.7	35
88	Investigation into the Interaction between Surface-Bound Alkylamines and Gold Nanoparticles. Langmuir, 2003, 19, 6277-6282.	1.6	469
89	Lamellar multilayer hexadecylaniline-modified gold nanoparticle films deposited by the Langmuir-Blodgett technique. Journal of Chemical Sciences, 2003, 115, 185-193.	0.7	6
90	Water-dispersible nanoparticles via interdigitation of sodium dodecylsulphate molecules in octadecylamine-capped gold nanoparticles at a liquid-liquid interface. Journal of Chemical Sciences, 2003, 115, 679-687.	0.7	12

#	Article	IF	CITATIONS
91	Phase transfer of silver nanoparticles from aqueous to organic solutions using fatty amine molecules. Journal of Colloid and Interface Science, 2003, 264, 396-401.	5.0	156
92	First results of the CAKE experiment. Radiation Measurements, 2003, 36, 335-338.	0.7	4
93	Moon and Sun shadowing effect in the MACRO detector. Astroparticle Physics, 2003, 20, 145-156.	1.9	29
94	Highly Oriented Gold Nanoribbons by the Reduction of Aqueous Chloroaurate Ions by Hexadecylaniline Langmuir Monolayers. Chemistry of Materials, 2003, 15, 17-19.	3.2	79
95	Gold Nanoparticles Assembled on Amine-Functionalized Naâ^'Y Zeolite:Â A Biocompatible Surface for Enzyme Immobilization. Langmuir, 2003, 19, 3858-3863.	1.6	90
96	Formation of Water-Dispersible Gold Nanoparticles Using a Technique Based on Surface-Bound Interdigitated Bilayers. Langmuir, 2003, 19, 1168-1172.	1.6	124
97	Morphology of BaSO4 Crystals Grown on Templates of Varying Dimensionality:  The Case of Cysteine-Capped Gold Nanoparticles (0-D), DNA (1-D), and Lipid Bilayer Stacks (2-D). Crystal Growth and Design, 2002, 2, 197-203.	1.4	37
98	Synthesis of Ag/Pd Nanoparticles and Their Low-Temperature Alloying within Thermally Evaporated Fatty Acid Films. Journal of Physical Chemistry B, 2002, 106, 297-302.	1.2	47
99	Growth of Calcium Carbonate Crystals within Fatty Acid Bilayer Stacks. Langmuir, 2002, 18, 6075-6080.	1.6	56
100	Crystallization of SrCO3 within thermally evaporated fatty acid films: unusual morphology of crystal aggregates. CrystEngComm, 2001, 3, 81.	1.3	7
101	Morphology of BaSO4 crystals grown at the liquid?liquid interface. CrystEngComm, 2001, 3, 213.	1.3	4
102	DNA-mediated electrostatic assembly of gold nanoparticles into linear arrays by a simple drop-coating procedure. Applied Physics Letters, 2001, 78, 2943-2945.	1.5	81
103	Low temperature crystalline Ag–Ni alloy formation from silver and nickel nanoparticles entrapped in a fatty acid composite film. Applied Physics Letters, 2001, 79, 3314-3316.	1.5	21
104	Sequential Electrostatic Assembly of Amine-Derivatized Gold and Carboxylic Acid-Derivatized Silver Colloidal Particles on Glass Substrates. Langmuir, 2000, 16, 6921-6926.	1.6	76
105	Amphoterization of Colloidal Gold Particles by Capping with Valine Molecules and Their Phase Transfer from Water to Toluene by Electrostatic Coordination with Fatty Amine Molecules. Langmuir, 2000, 16, 9775-9783.	1.6	64
106	Phase Transfer of Aqueous CdS Nanoparticles by Coordination with Octadecanethiol Molecules Present in Nonpolar Organic Solvents. Langmuir, 2000, 16, 9299-9302.	1.6	44
107	Microanalysis of uranium in Antarctica soil samples using fission track method. Journal of Radioanalytical and Nuclear Chemistry, 1995, 191, 381-386.	0.7	5
108	Trace uranium analysis of water from the south-west coastal region of India. Journal of Radioanalytical and Nuclear Chemistry, 1994, 178, 245-251.	0.7	7